THE IMPACT OF A DENSE CANOPY ON THE WIND PROFILE AND EVOLUTION OF THE BOUNDARY LAYER

Ian N. Harman* and John J. Finnigan

CSIRO Marine and Atmospheric Research, Canberra, Australia

1. INTRODUCTION

It has long been known that the standard surface layer flux-gradient relationships fail in a roughness sublayer (RSL) close to and within tall canopies. However there are a number of important applications where such approaches are still routinely used, for instance in operational numerical weather prediction, global climate and atmospheric dispersion models. Furthermore, due to practical reasons, most measurements made at long term flux stations are made in the RSL so a consistent theory for this region is needed. Here we address this problem by reconsidering simple one-dimensional, mixing length based models for the mean flow within and above a dense canopy in light of the mixing layer analogy for the flow at canopy top (Raupach et al., 1996).

2. MODEL

We consider the mean wind speed profile through a horizontally homogeneous, uniform, deep and dense canopy, where 'dense' is defined to mean that all momentum is absorbed through canopy drag. We consider that the flow is comprised of two coupled components. Firstly, within the canopy, stress divergence balances foliage drag, which is taken to be proportional to the square of the mean wind speed, to give the well known exponential form for the mean wind speed profile (e.g. Cionco, 1963). This can be expressed as

$$U(z) = U_h \exp\left\{ z / 2\beta^2 L_c \right\}, \qquad (1)$$

where $\beta = u_* / U_h$, u_* is the friction velocity at canopy top, U_h the wind speed at canopy top, L_c a length scale associated with the canopy density and where the co-ordinate system has its vertical origin at the canopy top.

Secondly, above the canopy the mean wind speed profile takes the usual surface layer form but modified by the existence of the roughness sublayer, i.e.

$$\frac{dU}{dz} = \frac{u_*}{\kappa(z+d_t)} \Phi_m = \frac{u_*}{\kappa(z+d_t)} \phi_m \hat{\phi}, \quad (2)$$

Corresponding author address: Ian N. Harman, CSIRO Marine and Atmospheric Research, GPO Box 3023, Canberra, ACT, 2601. Australia. e-mail: ian.harman@csiro.au

where ϕ_m is the standard surface layer flux-gradient relationship and $\hat{\phi}$ is an analogous function representing the increased mixing in the roughness sublayer (e.g. Garratt 1980) and whose value lies between 0 and 1. The displacement height, d_t, measured *downwards from the canopy top*, is given as the centre of the turning moment associated with the aerodynamic drag in the canopy (e.g. Jackson 1981), i.e.

$$d_t = \beta^2 L_c. \qquad (3)$$

Integrating Equation (4) gives a mean wind speed profile above the canopy of the form

$$U(z) = \frac{u_*}{\kappa}\left[\ln\left(\frac{z+d_t}{z_{0m}}\right) - \psi_m\left(\frac{z+d_t}{L_{MO}}\right) + \hat{\psi} \right], (4)$$

where ψ_m is the usual integrated form of the flux-gradient relationship *including* the correction at $z = -d_t + z_{0m}$, and $\hat{\psi}$ is the corresponding term from the roughness sublayer function given by

$$\hat{\psi}(z) = \int_{z+d_t}^{\infty} \frac{\phi_m(z')\left(1 - \hat{\phi}(z')\right)}{z'} dz' \qquad (5)$$

The two components are coupled together by equating the wind speed and its gradient at canopy top, whereby

$$\phi_{m,z=0}\,\hat{\phi}_{z=0} = \kappa d_t / 2\beta^3 L_c = \kappa / 2\beta, \qquad (6)$$

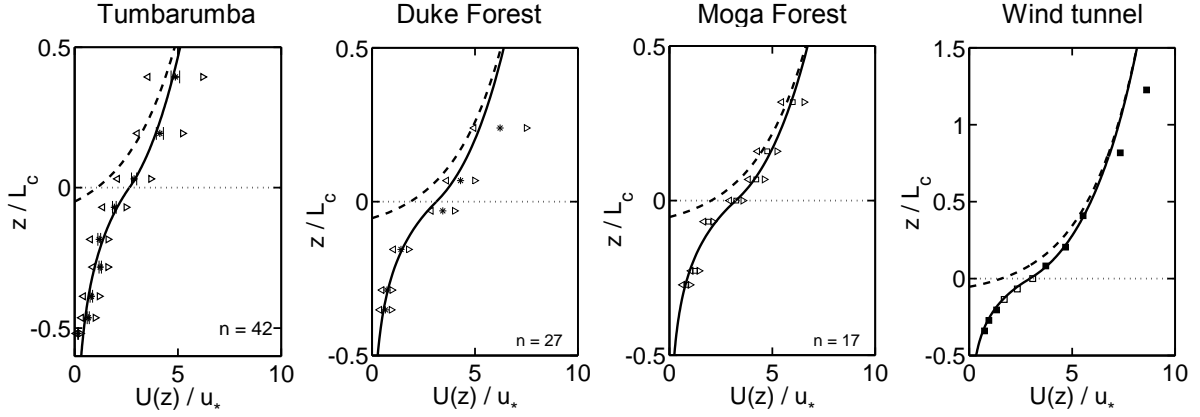$$z_{0m} = d_t \exp\left\{ -\kappa/\beta - \psi_{m,z=0} + \hat{\psi}_{z=0} \right\}. \qquad (7)$$

Equation (7) for the roughness length, z_{0m}, is a direct consequence of the continuity of the wind profile at canopy top and, crucially, implies that the roughness length associated with a dense canopy varies systematically with diabatic stability.

2.1 The roughness sublayer influence

The roughness sublayer over tall dense canopies is characterised by large-scale coherent motions centred on the canopy top. The mixing layer analogy (Raupach et al. 1996) provides a mechanistic explanation and a vertical length scale, the vorticity thickness at canopy top, for these coherent motions. Equating this vertical length scale to the length scale associated with changes in the roughness

Figure 1. Comparison of model predictions and observations from the three forests in (near-) neutral conditions. Markers give the mean of the n profiles, triangles mark one standard deviation from the mean, solid line is the model prediction and dashed line the extrapolated surface layer profile. The LAI of the canopies increases from left to right from 2 to 3.5, that of the wind tunnel study is 3.7.

sublayer function $\left(\Delta\hat{\phi}/\hat{\phi}'\right)$ then allows a natural form for the roughness sublayer function to be found, namely

$$\hat{\phi}(z) = 1 - c_1 \exp\left\{-c_2\left(z + d_t\right)\big/2\beta^2 L_c\right\}. \quad (8)$$

c_2 is an order one constant which relates the two length scales and c_1 can be determined in terms of other parameters through Equation (4) as

$$c_1 = \left(1 - \frac{\kappa}{2\beta\,\phi_{m,z=0}}\right)\exp\left\{c_2/2\right\}. \quad (9)$$

Hence, given a value of β and c_2, the full wind speed profile within and above the canopy can be determined. In practice, c_2 takes the value 0.5 and β varies significantly with canopy density and diabatic stability (see Figure 4) and has to be obtained from observations.

There are a number of advantages of this form (8) of the roughness sublayer function over previous forms in the literature (e.g. Garratt 1980; 1983; Cellier and Brunet 1994; Raupach 1994). These are, firstly, that the density of the canopy appears naturally in this form. Secondly, the function *asymptotes* to the correct limit of 1 with increasing height and is not forced to that value. Consequently, there is no unphysical discontinuity in the gradient of $\hat{\phi}$ at any height. Finally, Equation (8) does not require the *a priori* specification of the depth of the roughness sublayer or surface layer.

3. DATA

Sonic anemometry data from three sites are used to provide mean wind speed profiles. These are, firstly, hourly-averages over a fifteen week period from Tumbarumba in south-eastern Australia. Secondly, half-hourly averages from an intensive observation campaign at the Blackwood Division of Duke Forest, North Carolina, and finally half-hourly averages from an intensive observation campaign at Moga Forest, south-eastern Australia. Together these three forests represent a range of LAI from 2 to 3.5, and profiles are available across a wide range of diabatic stabilities

4. RESULTS

4.1 Variation with canopy density

Figure 1 shows vertical profiles of the wind speed for each of the three canopies in near-neutral conditions, together with observations taken from the wind tunnel study of Brunet et al. (1994). For each canopy, the value of the length scale L_c has been determined by parameter fitting to the within-canopy section of an independent subset of profiles. In each panel the central markers are the mean of the n observed profiles and the triangles mark one standard deviation from the mean. The solid line in each plot is the model prediction and the dashed line the extrapolation of the surface layer profile. In all panels the vertical scale is normalised by the length scale L_c (the height of the canopy does not enter the model for a deep, dense canopy) and the dotted line marks the canopy top.

There is excellent agreement between model predictions and observations as shown in Figure 1. A portion of this agreement arises from the use of the observed β but the good subsequent agreement through the full vertical extent of the profile illustrates the appropriateness of the vertical scaling used. The influence of the roughness sublayer can be clearly seen in each of the profiles as the deviation from the extrapolated surface layer profile above the canopy. This in turn suggests
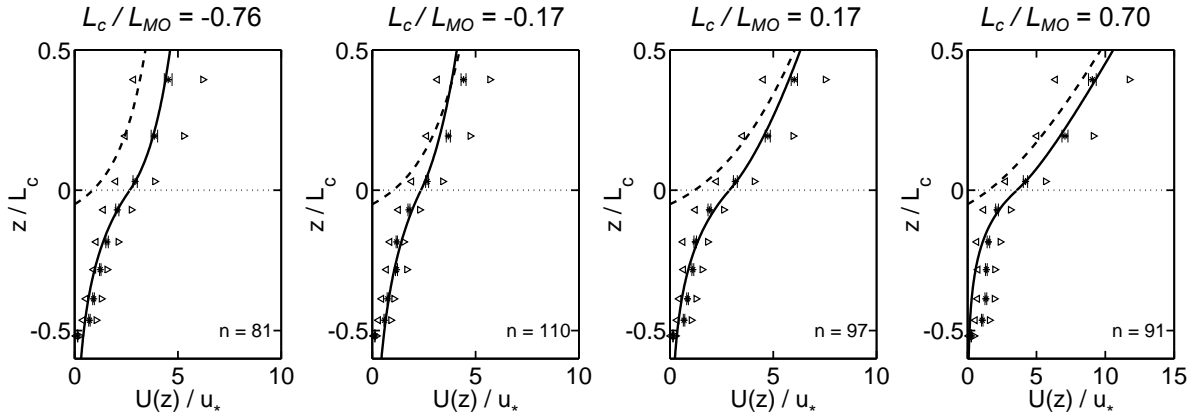
Figure 2. Comparison of model predictions and observations from Tumbarumba in non-neutral conditions. Solid line is the model prediction; dashed line, the surface layer profile calculated assuming the displacement height and roughness length take values as in neutral conditions. Markers give the mean of the n profiles, with error bars the standard error of the mean; triangles mark one standard deviation from the mean.

that even the uppermost observation point in each of the forest profiles may not be statistically free of roughness sublayer effects. There are small differences between the observations and model predictions, particularly with the profile from Duke Forest, but these can largely be explained by site specific characteristics such as variation in canopy density and limited fetch.

4.2 Variation with diabatic stability

Figure 2 shows vertical wind profiles from the Tumbarumba campaign averaged according to diabatic stability (as classified by the ratio L_c / L_{MO}, with L_{MO} the Obukhov length, above each panel). The observations show that there is a significant variation with diabatic stability of the wind profile both within and above the canopy, even over this high roughness surface. There is also generally good agreement between the observations and model predictions across the full range of diabatic stabilities. The main exception is the underestimate of the wind speed within the canopy in highly stable conditions. However, in these circumstances we expect a drainage current due to the small (4°) slope at the site.

In each panel the dashed line is now the surface layer profile obtained incorporating the effects of diabatic stability, but where the displacement height and roughness length take values as in neutral conditions. This profile shows significant differences to the observations and to the full model in slope and particularly in offset. These differences arise due to the variation with diabatic stability of the displacement height, through a systematic variation of β, and roughness length, through both the variation of β and the explicit variation in Equation (5). Across the range of diabatic

stability shown here β varies by a factor of 2, leading the displacement height, as given by (3), to vary by a factor 4 and the roughness length by a factor of approximately 2.5.

The roughness sublayer is found to have the largest impacts on the mean wind speed profile in near-neutral and slightly stable conditions. This is because the mixing layer instability, which we postulate gives rise to the coherent structures in the flow (Raupach et al. 1996), is dependent on the degree of inflection in the mean wind speed profile at canopy top. In highly stable conditions the buoyant suppression of motions outweighs the increased shear in the profile at canopy top. In unstable conditions, buoyant motions have smoothed out the inflection in the profile at canopy top so leading to a reduction in the impact of the mixing layer eddies.

5. IMPLICATIONS

5.1 Parameter estimation from profiles
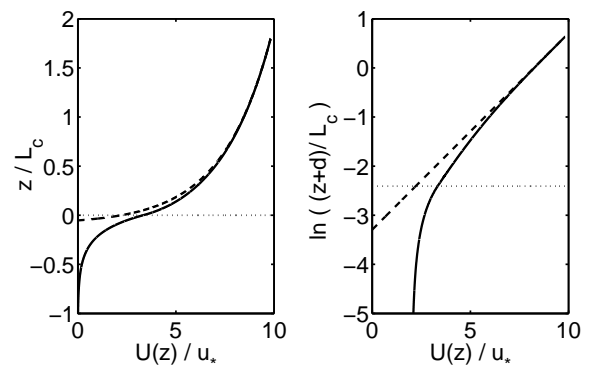
Figure 3. Mean wind speed profiles expressed on natural (left) and log (right) vertical scales. Solid line is the model profile; dashed line is the extrapolated surface layer profile.
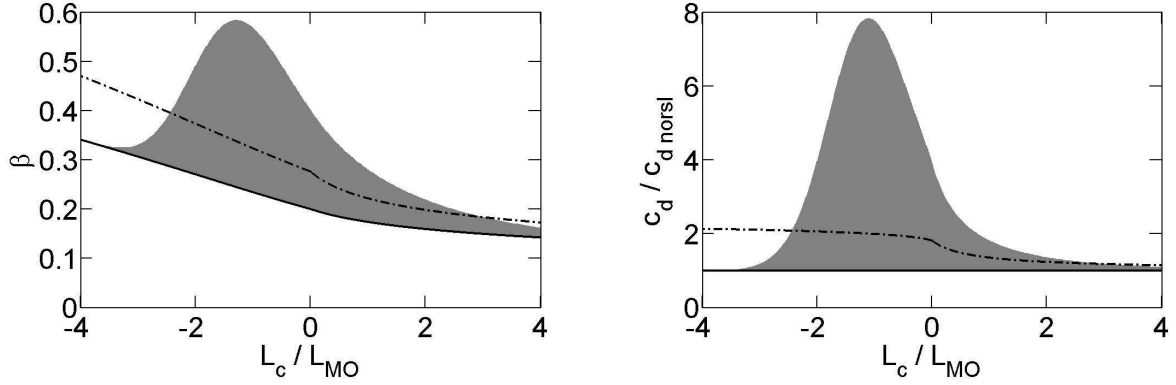
Figure 4. Left panel: Spread of the observed β from the Duke Forest campaign. The solid line represents the no RSL limit (observations which fell below this limit are not included in the composites); dashed line, a fit to the observations in the range $-1 < L_c / L_{MO} < 1$. Right panel: Resulting spread of the total drag coefficient, based on the wind speed at 10m above the canopy, normalised by the no roughness sublayer case.

A commonly used method to estimate profile parameters such as the displacement height and roughness length is to obtain these from an observed mean wind speed profile. This method requires the existence, when plotted on a log-z scale, of a linear section of the profile which is as such identified as the surface layer.

However, as the right panel of Figure 3 shows, the exponential nature of the $\hat{\phi}$ function ensures that the wind speed profile in the roughness sublayer also appears (approximately) linear on such a vertical scale, but with a different slope. It follows that there is potential for the false identification of the surface layer from observed profiles which do not extend into the surface layer proper and hence potential for the incorrect estimation of profile parameters.

5.2 Estimation of total drag from a single wind speed observation

To this point we have addressed the question of determining the wind profile given information on the friction velocity, diabatic stability and the canopy properties. A more common question is to determine the friction velocity, or equivalently total drag or drag coefficient, given information about the wind speed at a level above the canopy, diabatic stability and canopy properties. Such questions form the core of surface exchange schemes within numerical weather prediction and SVAT models (e.g. Physick and Garratt 1995; Graefe 2004). How would the inclusion of a roughness sublayer influence such calculations?

Defining a drag coefficient as

$$u_*^2 = c_d(z)U^2(z) \qquad (10)$$

Equation (4) can be inverted to give c_d at any height given a value of β and L_c. The left panel

Figure 4 shows the observed spread of β from the Duke Forest campaign; the solid line is the no roughness sublayer case and the dash-dotted line a fit through the observations in near-neutral conditions. Similar variation is seen in the other campaigns. The right panel of Figure 4 shows the corresponding spread of c_d at 10m above the canopy normalised by that calculated with no roughness sublayer included. While the large fractional increases in unstable conditions may be discounted statistically, this shows that the difference between including and neglecting the roughness sublayer could easily be a factor of 2 in terms of the total drag per unit 10m wind speed across a wide range of diabatic stabilities. Including, both in formulation and calibration, the roughness sublayer, and its variation with diabatic stability, into numerical weather prediction would therefore have significant impacts on the predicted dispersion characteristics and evolution of the boundary layer within these models.

6. CONCLUSIONS

Finally, we conclude that

1. The failure of the standard surface layer flux-gradient relationships can be related to the existence of large-scale coherent structures within the flow whose impact is not accounted for in the standard relationships.

2. The vertical length scale of the coherent structures, identified through the mixing layer analogy (Raupach et al. 1996), allows the formulation of a roughness sublayer function which accounts for their influence on the mean wind speed profile, and that this function is valid across a range of diabatic stabilities and canopy densities.

3. By including the coupling of the flow within and above the canopy, profile parameters such as the displacement height and roughness length are found to vary systematically with diabatic stability.

4. The roughness sublayer has a significant effect on the wind speed profile, but one which can be hidden by the profile curvature near the surface. It is however important to recognise the impacts of the roughness sublayer both in terms of profile parameter estimation and, in particular, within the formulation and calibration of surface exchange schemes within numerical weather prediction models.

Further work is required to establish whether the approach employed here can be applied to other variables, for instance the mean profiles of a scalar or the turbulent variances.

7. REFERENCES

Brunet, Y., Finnigan, J.J. and Raupach, M.R., 1994: A wind-tunnel study of air flow in waving wheat: Single-point velocity statistics. *Bound.-Layer Meteor.*, **70**, 95–132.

Cellier, P. and Brunet, Y., 1992: Flux-gradient relationships above tall plant canopies. *Agric. For. Meteor.*, **58**, 93–117.

Cionco, R.M., 1965: A mathematical model for air flow in a vegetative canopy. *J. Appl. Meteor.*, **4**, 517–522.

Garratt, J.R., 1980: Surface influence on vertical profiles in the atmospheric surface layer. *Quart. J. Roy. Meteor. Soc.*, **106**, 803–819.

Garratt, J.R., 1983: Surface influence upon vertical profiles in the nocturnal boundary layer. *Bound.-Layer Meteor.*, **26**, 69–80.

Graefe, J., 2004: Roughness sublayer corrections with emphasis on SVAT applications. *Agric. For. Meteor.*, **124**, 237–251.

Jackson, P.S., 1981: On the displacement height in the logarithmic velocity profile. *J. Fluid Mech.*, **111**, 15–25.

Raupach, M.R., 1994: Simplified expressions for vegetation roughness length and zero-plane displacement as functions of canopy height and area index. *Bound.-Layer Meteor.*, **71**, 211–216.

Raupach, M.R., Finnigan, J.J. and Brunet, Y., 1996: Coherent eddies and turbulence in vegetation canopies: The mixing layer analogy. *Bound.-Layer Meteor.*, **78**, 351–382.

Physick, W.L. and Garratt, J.R., 1995: Incorporation of a high-roughness lower boundary into a mesoscale model for studies of dry deposition over complex terrain. *Bound.-Layer Meteor.*, **74**, 55–71.